Tectonophysics xxx (2010) xxx–xxx

Contents lists available at ScienceDirect

Tectonophysics

journal homepage: www.elsevier.com/locate/tecto

The effect of asymmetric damage on dynamic shear rupture propagation II: With mismatch in bulk elasticity

H.S. Bhat [a,b,*], R.L. Biegel [a], A.J. Rosakis [b], C.G. Sammis [a]

[a] Department of Earth Sciences, 3651 Trousdale Parkway Los Angeles, CA 90089, USA
[b] Graduate Aerospace Laboratories, 1200 E. California Blvd., Pasadena, CA 91125, USA

ARTICLE INFO

Article history:
Received 1 October 2009
Received in revised form 27 February 2010
Accepted 24 March 2010
Available online xxxx

Keywords:
Dynamic shear rupture
Bimaterial ruptures
Damage mechanics
Supershear

ABSTRACT

We investigate asymmetric rupture propagation on an interface that combines a bulk elastic mismatch with a contrast in off-fault damage. Mode II ruptures propagating on the interface between thermally shocked (damaged) Homalite and polycarbonate plates were studied using high-speed photographs of the photoelastic fringes. The anelastic asymmetry introduced by damage is defined by 'T' and 'C' directions depending on whether the tensile or compressive lobe of the rupture tip stress concentration lies on the damaged side of the fault. The elastic asymmetry is commonly defined by '+' and '−' directions where '+' is the direction of displacement of the more compliant material. Since damaged Homalite is stiffer than polycarbonate, the propagation directions in our experiments were 'T+' and 'C−'. Theoretical and numerical studies predict that a shear rupture on an elastic bimaterial interfaces propagates in the '+' direction at the generalized Rayleigh wave speed or in some numerical cases at the P-wave speed of the stiffer material, P_{fast}. We present the first experimental evidence for propagation at P_{fast} in the '+' direction for the bimaterial system undamaged Homalite in contact with polycarbonate. In the '−' direction, both theory and experiments find ruptures in elastic bimaterials propagate either at sub-shear speed or at the P-wave speed of the softer material, P_{slow}, depending on the loading conditions. We observe that the off-fault damage effect dominates the elastic bimaterial effect in dynamic rupture propagation. In the 'C−' direction the rupture propagates at sub-shear to supershear speeds, as in undamaged bimaterial systems, reaching a maximum speed of P_{slow}. In the 'T+' direction however the rupture propagates at sub-shear speeds or comes to a complete stop due to increased damaged activation (slip and opening along micro-cracks) which results in a reduction in stored elastic potential energy and energy dissipation. Biegel et al. (2010-this issue) found similar results for propagation on the interface between Homalite and damaged Homalite where rupture speeds were slowed or even stopped in the 'T−' direction but were almost unaffected in the 'C+' direction.

1. Introduction

Rupture propagation in most large earthquakes is asymmetric. McGuire et al. (2002) found that about 80% of the large shallow earthquakes that have occurred since 1994 were characterized by unilateral propagation over the fault plane. As they note, a simple geometrical explanation is that large earthquakes are "characteristic" in that their size is determined by the size of the fault segment on which they occur. Such earthquakes would be truly bilateral only if nucleation occurred near the center of the characteristic segment. However, there are structural features of the fault zones themselves that favor asymmetric dynamic propagation, which include both a contrast in elastic stiffness and a contrast in fracture damage across the slip plane.

Large displacements on major faults often bring rocks with different elastic constants into contact across the fault plane. Theoretical and experimental studies (Weertman, 1980; Harris and Day, 1997; Ben-Zion, 2001; Rice, 2001; Rosakis et al., 2007, and references therein) have found that a contrast in the elastic stiffness of wall rocks produces asymmetric propagation of mode II ruptures. The rupture tip that propagates in the direction of motion of the less stiff (lower velocity) wall rock (termed the '+' direction) travels at a different velocity than the tip propagating in the opposite '−' direction. This asymmetry has been ascribed to a dynamic reduction in normal stress at the crack tip propagating in the '+' direction (Rice, 2001). The exact nature of the directionality is also sensitive to the details of static and dynamic friction on the fault plane. Generalized Rayleigh waves can be sustained on an interface which separates materials with less than about a 35% difference in shear wave speeds (as is the case for most natural faults). These waves of frictionless contact propagate at a speed, c_{GR}, called the generalized Rayleigh wave speed (Rice, 2001).

Weertman (1980) found an analytic solution for a dislocation-like sliding pulse propagating with a velocity equal to c_{GR} along an interface governed by Amonton–Coulomb friction. However, Ranjith and Rice (2001) demonstrated that classical Amonton–Coulomb friction is

* Corresponding author. Department of Earth Sciences, 3651 Trousdale Parkway Los Angeles, CA 90089, USA.
E-mail address: hbhat@usc.edu (H.S. Bhat).

0040-1951/$ – see front matter © 2010 Elsevier B.V. All rights reserved.
doi:10.1016/j.tecto.2010.03.016

inadequate for this problem since periodic perturbations to steady sliding grow unbounded for a wide range of frictional coefficient and bimaterial properties (Renardy, 1992; Adams, 1995). For bimaterial systems where generalized Rayleigh waves exist, Ranjith and Rice (2001) demonstrate that unstable periodic modes of sliding appear for all values of the friction coefficient. The problem is regularized by utilizing an experimentally based frictional law (Prakash and Clifton, 1993), in which the shear strength evolves continuously with time following an abrupt change in normal stress (Cochard and Rice, 2000; Ranjith and Rice, 2001). In such a case, the problem becomes well-posed and generic self-sustained pulse solutions exist while numerical convergence through grid size reduction is achieved Cochard and Rice (2000); Coker et al. (2005). However, despite the fact that this special frictional law provides regularization, self-sustained slip pulses may still grow in magnitude with time as demonstrated numerically by Ben-Zion and Huang (2002).

Two types of steady, self-sustained pulses were discovered theoretically by Ranjith and Rice (2001). Consistent with Weertman (1980), the first type corresponds to rupture growth in the direction of sliding of the lower wave speed material. This direction is referred to in the literature (Ben-Zion, 2001; Rice, 2001) as the '+' direction and sometimes as the "preferred" direction (Ben-Zion, 2001). These type I pulses always propagate with a steady velocity, $v_r = c_{GR}$. The second type of self-sustained rupture propagates in the opposite '−' direction. These ruptures always propagate with a steady velocity that is slightly lower than the P-wave speed of the material with the lesser wave speed $v_r = P_{slow}$. Type II ruptures are generated for sufficiently high values of the coefficient of friction (Ranjith and Rice, 2001) and are less unstable than the ruptures described above (Cochard and Rice, 2000). In addition Ranjith and Rice (2001) show that for sufficiently large values of friction coefficient, f, a family of non-growing supersonic, i.e. $v_r = P_{fast}$, interfacial wave solutions also exist in the '+' direction.

Numerical simulations by Cochard and Rice (2000), which utilized the modified Prakash–Clifton Law but assumed a constant coefficient of friction, excited regularized self-sustained pulses of both types (c_{GR} in the '+' direction and P_{slow} in the '−'direction). As discussed by Rosakis et al. (2007) either type could be excited by fine tuning parameters in the friction law and the geometry of the nucleation zone, however a simultaneous excitation of both modes was never reported. A slip-weakening friction law, on the other hand, allows both types of sliding modes to propagate in opposite directions during the same rupture event in 2D (Harris and Day, 1997) and in 3D (Harris and Day, 2005). The results of these studies were also consistent with the early experiments of Xia et al. (2005). Shi and Ben-Zion (2006) did an extensive parameter study for 2D bimaterial ruptures with slip-weakening friction law and in addition to bilateral rupture also found that for large strength drop from static to dynamic friction the rupture in the '+' direction propagated at velocities approaching P_{fast}. Rubin and Ampuero (2007) found that slip-weakening friction under smooth loading conditions led to slightly asymmetrical bilateral growth whereas unilateral ruptures were produced under abrupt loading conditions that were too short to allow significant slip-weakening. They also found that (with regularization) when normal stress evolved with slip, the rupture in the '−' direction propagated at c_{GR} while the rupture in the '+' direction propagated at supershear speeds less than P_{slow}. This trend was reversed when normal stress evolved with time rather than slip. Using a velocity weakening friction law with state dependence, Ampuero and Ben-Zion (2008) showed that large scale pulses associated with velocity weakening friction and small scale wrinkle-like pulses associated with bimaterial effects were generated. While the appearance of the former is quite robust, i.e. it is less sensitive to the details of normal stress regularization, stress heterogeneity and off-fault plastic yielding, the latter was extremely sensitive to the numerical and physical details of the problem.

The effect of elastic wave speed contrast on rupture velocity asymmetry and on transition to supershear speeds was experimentally explored by Xia et al. (2005). These experiments suggested that ruptures in the '+' direction propagated at the generalized Rayleigh wave speed of the interface while the same in the opposite, '−' direction, transitioned to supershear speed approaching P_{slow} which is in good agreement with the theoretical and numerical models. Recent experimental studies of mode II ruptures propagating on the interface between damaged and undamaged photoelastic Homalite plates found that fracture damage introduces an additional asymmetry beyond that due to the associated elastic contrast (Biegel et al., 2010-this issue). A rupture propagating in the direction for which the tensile lobe of the stress concentration at its tip moves through the damaged wall rock (which we term the 'T' direction) travels more slowly that a rupture traveling in the opposite 'C' direction for which compressive lobe travels through the damage. This asymmetry has been ascribed to an enhancement of anelastic slip on damage-fractures in the tensile lobe and its suppression in the compressive lobe. In fact, ruptures traveling in the 'C' direction appeared to be nearly unaffected by the damage (Biegel et al., 2010-this issue). While this is certainly true for high angles between the principal stress with the fault plane (the experimental configurations in this paper result in such angles ranging between 62° and 65°), it is possible for damage to occur in the compressive quadrant when the maximum compressive stress is inclined at very shallow angles to the fault.

In Biegel et al. (2010-this issue), the interface between damaged and undamaged Homalite is characterized by a contrast in both elastic stiffness and damage. This is in contrast with Xia et al. (2005) where only elastic mismatch and no damage was present. The direction of motion of the damaged Homalite is the 'C+' direction since damaged Homalite has a lower elastic stiffness than does undamaged Homalite and the rupture tip in this direction has its compressive stress lobe in the damage. The other crack tip travels in the 'T−' direction.

In this paper we explore mode II propagation on the interface between damaged Homalite and undamaged polycarbonate. See Fig. 1 where the situation describes a fault with right-lateral sense of slip. Since polycarbonate is even less stiff than damaged Homalite, the direction in which the polycarbonate moves is 'T+'; termed '+' because it is the direction in which the less stiff polycarbonate moves and (T) because the crack tip moving in this direction places the damaged Homalite in tension. The other tip propagates in the 'C−' direction. In this case the direction favored by elasticity is opposite to the direction favored by the damage.

2. Experimental apparatus and procedures

We used the same apparatus and followed the same procedures described by Xia et al. (2004, 2005), Rosakis (2002) and Biegel et al.

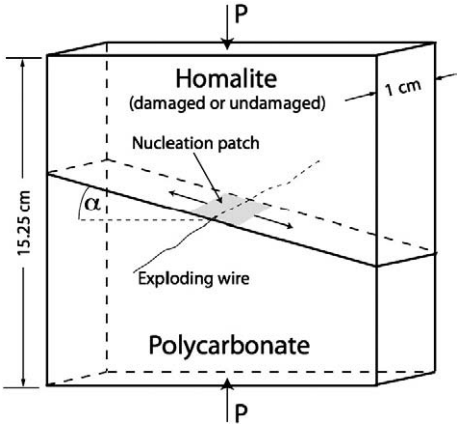

Fig. 1. Sample geometry. Homalite plate (damaged or undamaged) in frictional contact with a polycarbonate plate along a fault at an angle α and loaded in uniaxial compression P. Exploding wire reduces normal stress on a fault patch which nucleates a bilateral rupture.

Please cite this article as: Bhat, H.S., et al., The effect of asymmetric damage on dynamic shear rupture propagation II: With mismatch in bulk elasticity, Tectonophysics (2010), doi:10.1016/j.tecto.2010.03.016

(2008, 2010-this issue) Square plates of the transparent photoelastic polymers Homalite and polycarbonate (15.25 cm × 15.25 cm × 1 cm) were bisected by a saw-cut fault at an angle α to one edge. The contacting faces were lapped with #220 sandpaper. Mean surface roughness was measured to be 2 μm using a digital mechanical profilometer. As in Xia et al. (2005), one half of a polycarbonate plate was placed in contact with one half of a Homalite plate as shown in Fig. 1. The samples were loaded with uniaxial stress P and a dynamic rupture was nucleated by using a high voltage pulse to explode a wire across the center of the fault plane. The explosion reduces normal stress on a patch of the fault approximately 1 cm long thereby nucleating a rupture which, in most cases, propagates bilaterally. The voltage pulse also triggers high-speed digital cameras which take a series of pictures of the propagating rupture using transmitted polarized laser light that resolves the photoelastic fringes produced by the spatial gradients in shear stress (Fig. 2). The experiments described here differ from those in Xia et al. (2005) in that our surfaces were significantly smoother and, in some experiments, the Homalite half plate was fracture damaged as shown in the inset in Fig. 2. Fracture damage was generated as described in Biegel et al. (2008, 2010-this issue) by using a razor knife to produce a grid of scratches approximately 2 mm apart (chosen simply for convenience rather than mimicking real earth damage density) oriented at $\pm 45°$ to the loading axis, and then dipping the plate in liquid nitrogen for 45 s. We did not explore cases involving damaged polycarbonate plates because this thermal shock procedure did not produce fracture damage in polycarbonate.

3. Elastic properties of Homalite, damaged Homalite and polycarbonate

The elastic properties of Homalite, damaged Homalite and polycarbonate are given in Table 1. The S wave speed in damaged Homalite was measured by Biegel et al. (2008). The corresponding P-wave speed and Poisson's ratio were estimated using the model for fracture damaged materials formulated by O'Connell and Budiansky (1974) as detailed in Biegel et al. (2008). The elastic moduli of these polymers are only about 5% of the comparable values for rock. The consequences of this reduced stiffness are a much smaller nucleation patch size and a much smaller value of R_0, the size of the process zone which determines the spatial extent of the crack-tip stress and velocity fields. These reductions in scale allow dynamic ruptures to be studies in the laboratory. The critical stress intensity factor and friction laws in the polymers are comparable to those in rock. Scaling laboratory observations to natural faults follows directly from Linear Elastic Fracture Mechanics and has been discussed in previous papers (Xia et al., 2004; Rice et al., 2005; Biegel et al., 2008, 2010-this issue).

Table 1
Material properties of sample materials.

	c_p (m/s)	c_s (m/s)	ν
Homalite	2498[a]	1200[a]	0.35[a]
Damaged Homalite	2200[b]	1000[c]	0.25[b]
Polycarbonate	2182[a]	960[a]	0.38[a]

[a] Rosakis et al. (2007).
[b] O'Connell and Budiansky, (1974).
[c] Biegel et al. (2008).

4. Measurement of rupture velocity

We measured the crack-tip position as a function of time from the isochromatic fringe patterns in successive high-speed digital images. These data were then fit with an interpolating cubic spline and a smoothing spline using the curve fitting toolbox in MATLAB®. The resulting fits were differentiated to obtain instantaneous rupture velocity as a function of time. Rupture velocities in the supershear

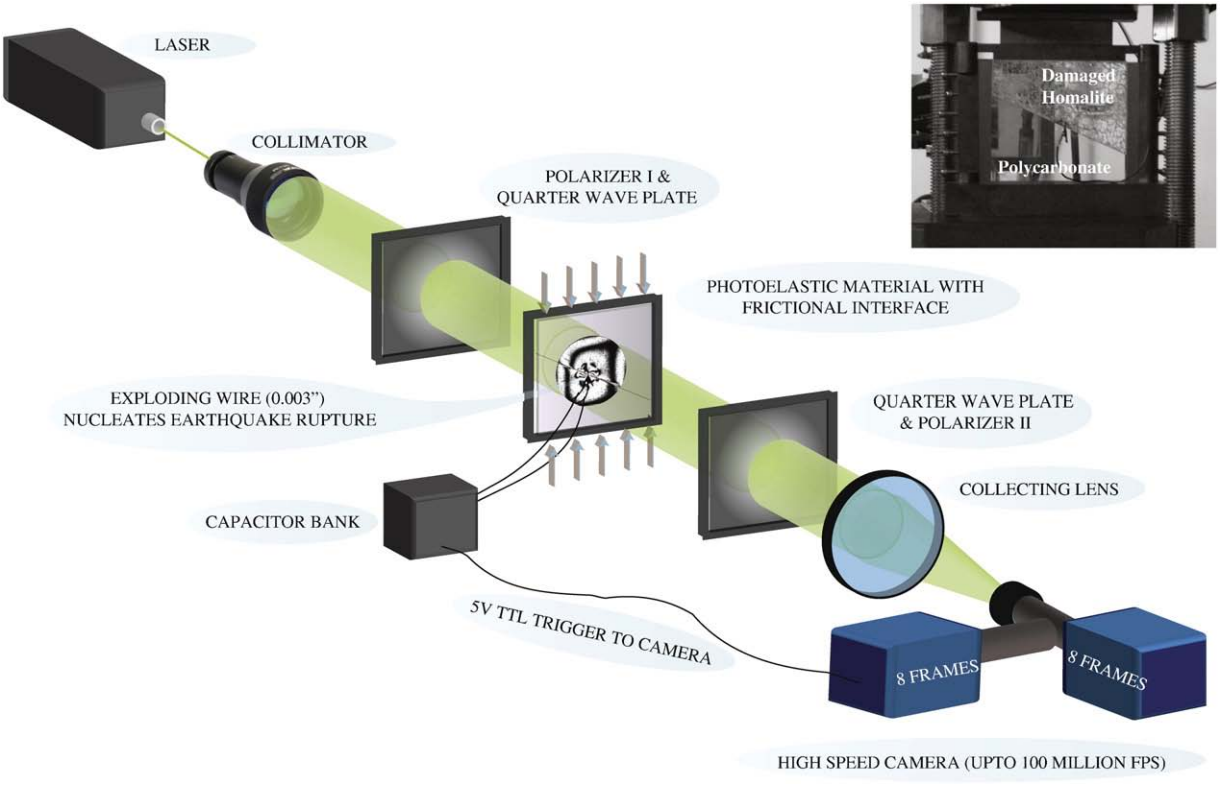

Fig. 2. Experimental apparatus used to photograph shear stress fringes in a photoelastic plates during dynamic rupture. Inset shows sample in loading frame used to apply uniaxial load P. The saw-cut fault separating Homalite (damaged or undamaged) and polycarbonate has a normal vector at an angle α to the load.

Please cite this article as: Bhat, H.S., et al., The effect of asymmetric damage on dynamic shear rupture propagation II: With mismatch in bulk elasticity, Tectonophysics (2010), doi:10.1016/j.tecto.2010.03.016

regime were checked by measuring the Mach angle, β, in Homalite and a^{PC} in polycarbonate in the photographs and using the relationship

$$\frac{v_r}{c_s} = \frac{1}{\sin\beta} = \left(\frac{c_s^{PC}}{c_s \sin\beta^{PC}}\right) = \frac{0.8}{\sin\beta^{PC}}. \quad (1)$$

Here c_s and c_s^{PC} are the S wave speeds of Homalite and polycarbonate respectively.

5. Mode II propagation on the boundary between elastic materials having different moduli

Before presenting our results for mode II propagation on the interface between damaged Homalite and polycarbonate, we first discuss propagation on the interface between undamaged Homalite and polycarbonate. This case was first explored by Xia et al. (2005) for uniaxial loads between 10 and 18 MPa and fault angles between 20° and 25°. They found that all ruptures in the '+' direction propagated at the generalized Rayleigh speed c_{GR}, which is a solution of following equation (Rice, 2001):

$$f(V) = \left(1-b_1^2\right)a_1 G_2 D_2 + \left(1-b_2^2\right)a_2 G_1 D_1 = 0 \quad (2)$$

where $a_n = \sqrt{1-\left(V/c_p^n\right)^2}$, $b_n = \sqrt{1-\left(V/c_s^n\right)^2}$ and $D_n = 4a_n b_n - (1-b_n^2)^2$. In these expressions, V is the rupture speed, G_n are the rigidity of the two materials ($n=1,2$). For the velocities given in Table 1, $c_{GR} = 959$ m/s. Propagation in the '−' direction was slower than the Rayleigh wave speed at small loads and low fault angles but transitioned to a supershear speed equal to the P-wave speed in the slower material ($P_{slow} \equiv c_p^{PC}$) at larger loads and higher angles. This result is consistent with the observation of supershear propagation in the '−' direction during the 1999 Izmit earthquake in Turkey (Bouchon et al., 2001; Rosakis et al., 2007). Evidence of bimaterial contrast in this section of the North Anatolian Fault (Le Pichon et al., 2003) is consistent with the direction of supershear as established by the experiment.

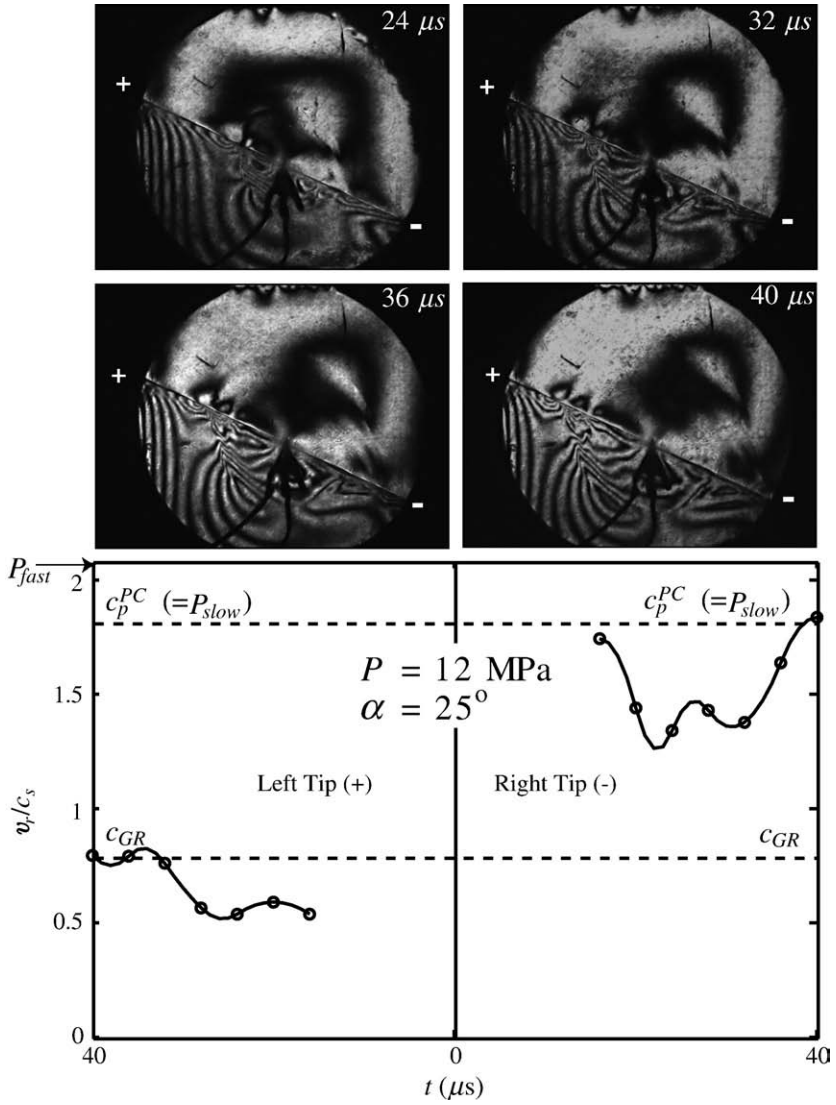

Fig. 3. Snapshots of isochromatic fringe pattern showing contours of maximum shear stress due to a dynamic shear rupture along a frictional interface between an undamaged Homalite plate above and an undamaged polycarbonate plate below. The applied load is $P=12$ MPa and the fault angle is $\alpha=25°$. Normalized rupture velocity v_r/c_s is plotted as a function of time for the left and right crack tips The left rupture tip travels in the '+' direction at the generalized Rayleigh speed. The right rupture tip transitions to supershear traveling at P_{slow}, the P-wave speed of the slower material (polycarbonate). Open circles indicate times at which the pictures were taken and the solid curves are the instantaneous rupture velocity found by differentiating cubic spline fits to the measured crack-tip positions as discussed in the text. The normalized P-wave speed in the faster material (Homalite) is 2.08 (the upper boundary of the graph). More fringes appear in the polycarbonate because it has a larger photoelastic constant.

Please cite this article as: Bhat, H.S., et al., The effect of asymmetric damage on dynamic shear rupture propagation II: With mismatch in bulk elasticity, Tectonophysics (2010), doi:10.1016/j.tecto.2010.03.016

We repeated (and extended) the Xia et al. (2005) measurements here because our fault surfaces were significantly smoother than those in their experiments and we would like a direct comparison between these undamaged cases and our experiments involving damage presented in the next section. Fig. 3 shows our results for $P=12$ MPa and $\alpha=25°$, which are identical to those in Xia et al. (2005). The rupture which propagated in the '−' direction transitioned to a supershear speed approaching $P_{slow}(\equiv c_p^{PC}$, the P-wave speed of polycarbonate), while the rupture in the '+' direction propagated at c_{GR}. When the load was increased to $P=15$ MPa (Fig. 4) the rupture which propagated in the '−' direction still transitioned to supershear with a velocity approaching P_{slow}. However, the rupture which propagated in the '+' direction also transitioned to a supershear speed approaching $P_{fast}(\equiv c_p$, the P-wave speed of Homalite). This is a new result and was not observed by Xia et al. (2005), even at $P=18$ MPa. Our observation of supershear in the '+' direction is probably the result of a shorter supershear transition length L in our experiments. Rosakis et al. (2007) demonstrated that L is inversely proportional to $P^{3/2}$ and directly proportional to the asperity size, implying a shorter transition length for our smoother surfaces. Measured mean surface roughness for Xia et al. (2005) samples was 25 μm (person. comm., K. Xia, 2007). The implication is that the ruptures observed by Xia et al. (2005) might also have transitioned to supershear at larger propagation distances and were missed by those earlier experiments.

An independent measure of the supershear rupture speed was obtained from Eq. (1) by measuring the angles β of the Mach cones on both the Homalite and polycarbonate sides and using the known elastic properties of in the two materials ($n=1,2$) given in Table 1. Measurements of rupture velocities obtained in this way are also plotted in Fig. 4 where they are seen to be consistent with the direct travel time measurements.

The results of Xia et al. (2005) and those found here for the elastic bimaterial pair of Homalite in contact with polycarbonate can be summarized as follows: (1) All ruptures were bilateral and no preferred direction was observed. (2) Depending on load and surface roughness, the rupture in the '+' direction propagates at either the generalized Rayleigh wave speed, c_{GR}, or at supershear speeds that approach $P_{fast}(\equiv c_p)$. (3) Depending on load and surface roughness, the rupture in the '−' direction propagates at either sub-shear speeds or it transitions to supershear speeds approaching $P_{slow}(\equiv c_p^{PC})$ For large enough P and/or high enough α, rupture in the '+' direction eventually transitions to supershear at P_{fast} while the rupture in the '−' direction eventually transitions to supershear at P_{slow}.

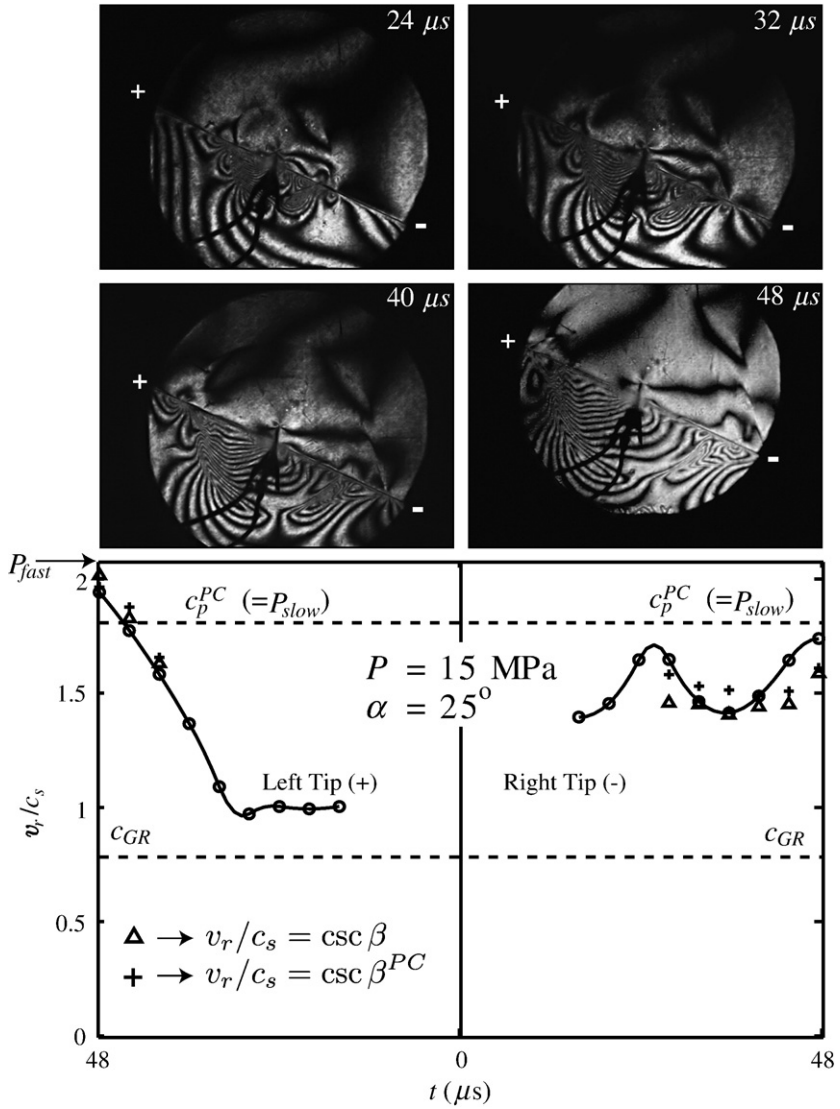

Fig. 4. Same as Fig. 3 except the applied load is $P=15$ MPa. Supershear velocities were checked by measuring the Mach angles β in the Homalite (open triangles) and β^{PC} in the polycarbonate (plus symbols) and using Eq. (1).

Please cite this article as: Bhat, H.S., et al., The effect of asymmetric damage on dynamic shear rupture propagation II: With mismatch in bulk elasticity, Tectonophysics (2010), doi:10.1016/j.tecto.2010.03.016

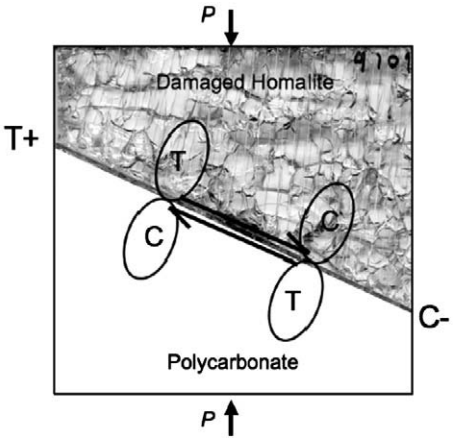

Fig. 5. Anelastic asymmetry results from the positions of the compressive and tensile stress concentration lobes of the two crack tips within the damaged Homalite. In the C direction, the compressive lobe is in the damage while in the T direction the tensile lobe is in the damage. Also shown are the '+' and '−' directions defined by the elastic contrast across the fault. The '+' direction is defined as the direction of motion of the more compliant wall rock (polycarbonate in this case).

As in Xia et al. (2005) we cannot discern whether the ruptures observed in our experiments where pulse-like, crack-like, or some complex combination of the two without additional measurements. However our measured rupture velocity evolutions not only confirm the previous results obtained by Xia et al. (2005) but also demonstrate a new mode of rupture propagation where the rupture in the '+' direction transitions to supershear speeds approaching P_{fast}. All of our results can be reconciled with existing analytical and numerical models. However, as shown by all the previous works on bimaterial ruptures, the final mode of propagation is highly sensitive to the nucleation conditions, the friction law governing slip on the interface and normal stress regularization mechanisms. These need to be explored numerically for the Homalite–polycarbonate bimaterial system.

6. Dynamic shear rupture on the interface between damaged Homalite and polycarbonate

To explore rupture directionality produced by a combination of asymmetric off-fault damage and a mismatch in bulk elasticity, we conducted a series of experiments in which ruptures propagated on the interface between damaged Homalite and polycarbonate. As illustrated

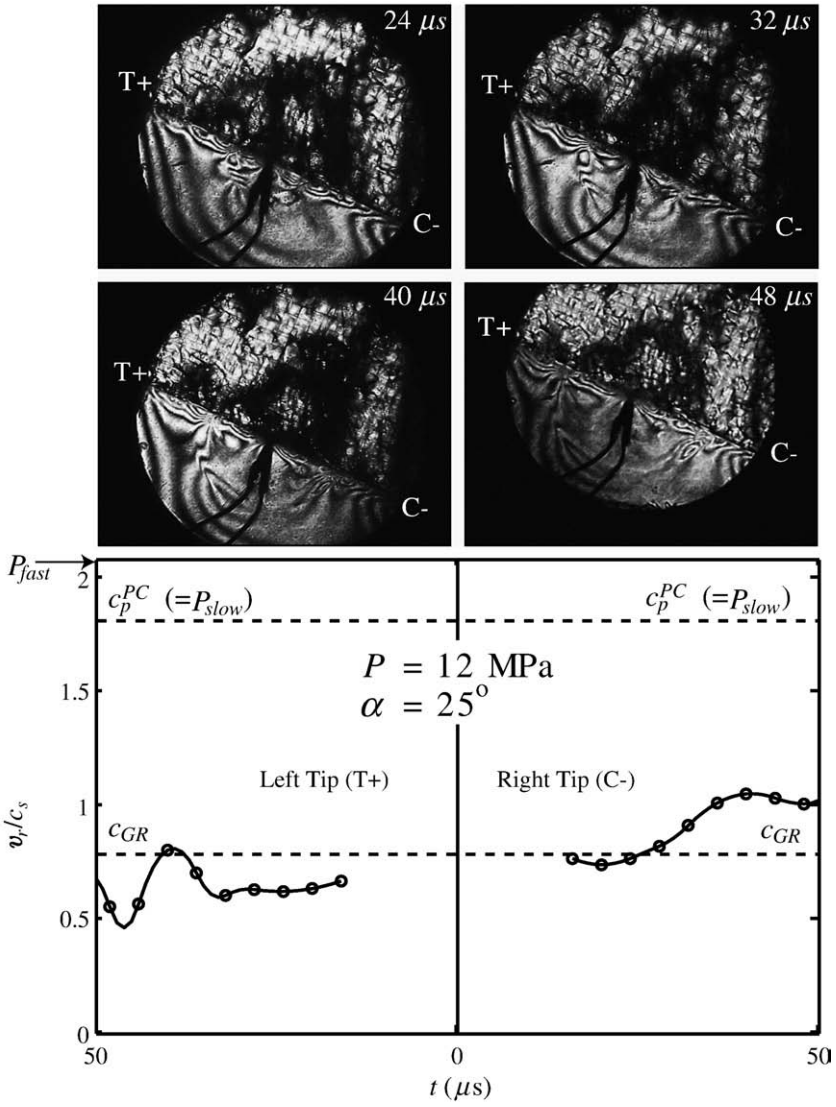

Fig. 6. The same as Fig. 3 except the bilateral shear rupture propagates along a frictional interface separating damaged Homalite above and undamaged polycarbonate below. The rupture tip propagating to the left 'T+' travels at speeds below c_{GR}, the generalized Rayleigh speed. The tip propagating to the right accelerates to speeds in excess of c_{GR}. All velocities are normalized to the shear wave speed in undamaged Homalite.

Please cite this article as: Bhat, H.S., et al., The effect of asymmetric damage on dynamic shear rupture propagation II: With mismatch in bulk elasticity, Tectonophysics (2010), doi:10.1016/j.tecto.2010.03.016

in Fig. 5, dynamic symmetry in these experiments is broken in two different ways. First, the contrast in elastic stiffness between damaged Homalite and polycarbonate introduces the elastic asymmetry described by the '+' and '−' propagation directions previously discussed. Second, the stress concentration at the rupture tip introduces an anelastic asymmetry based on whether the tensile or compressive lobe of the crack-tip stress concentration is on the damaged side of the interface. The side or direction of the rupture that places the compressive stress lobe, associated with the rupture tip, on the damaged material is called the 'C' side or direction. Similarly the 'T' side or direction corresponds to the rupture tip associated tensile stress field being on the damaged side. When this is combined with the '+' and '−' directions associated with material mismatch we get the following relevant combinations of sides or directions.

(i) 'C+' and 'T−' when a right-lateral rupture is bounded on top ($y>0$ domain) by an undamaged material of greater bulk elastic moduli which is discussed in part I of this paper (Biegel et al., 2010-this issue).
(ii) 'C−' and 'T+' when a right-lateral rupture is bounded on bottom ($y<0$ domain) by an undamaged material of lower bulk elastic moduli which is discussed in this paper. These asymmetries are illustrated in Fig. 5 which shows that ruptures propagating to the left are 'T+' while those propagating to the right are 'C−'.

More anelastic loss is expected at the rupture tip where the tensile lobe moves through the off-fault damage, which we term the 'T' direction. Less loss is expected in the opposite 'C' direction where the compressive lobe moves through the damage. The asymmetry arises because local tension relives normal stress to enhance frictional sliding on the fractures comprising the damage while local compression increases the normal load which suppressed sliding. Thus, for the rupture traveling in the 'C−' direction the micro-cracks have little or no activation leading to a bimaterial rupture between Homalite and polycarbonate in this direction. In contrast, along the 'T+' direction, the rupture plane is bounded by polycarbonate and damaged Homalite, whose elastic moduli is varying spatio-temporally with propagating rupture due to the activation of micro-cracks from the dynamic stress field associated with the rupture.

Experiments with two different combinations of uniaxial load are presented here: $P=12$ MPa; $\alpha=25°$ and $P=15$ MPa; $\alpha=25°$. Results for the case $P=12$ MPa and $\alpha=25°$ are given in Fig. 6. The effect of damage is evident in the 'T+' direction where the rupture propagated at an average speed below c_{GR}. In the 'C−' direction the rupture propagated at sub-shear speeds. When the load was increased to

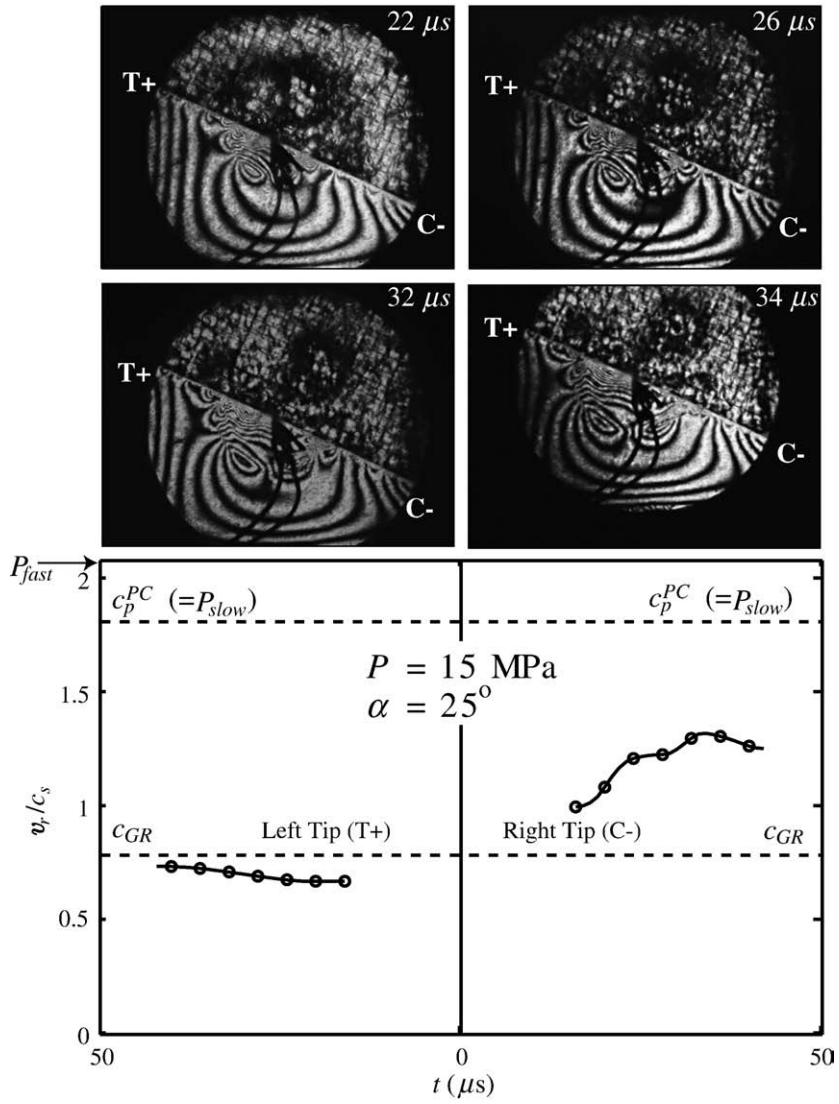

Fig. 7. Same as Fig. 6 except the applied load is $P=15$ MPa. The left rupture tip 'T+' approaches c_{GR}. The right rupture tip 'C−' accelerates to velocities well above c_{GR}.

Please cite this article as: Bhat, H.S., et al., The effect of asymmetric damage on dynamic shear rupture propagation II: With mismatch in bulk elasticity, Tectonophysics (2010), doi:10.1016/j.tecto.2010.03.016

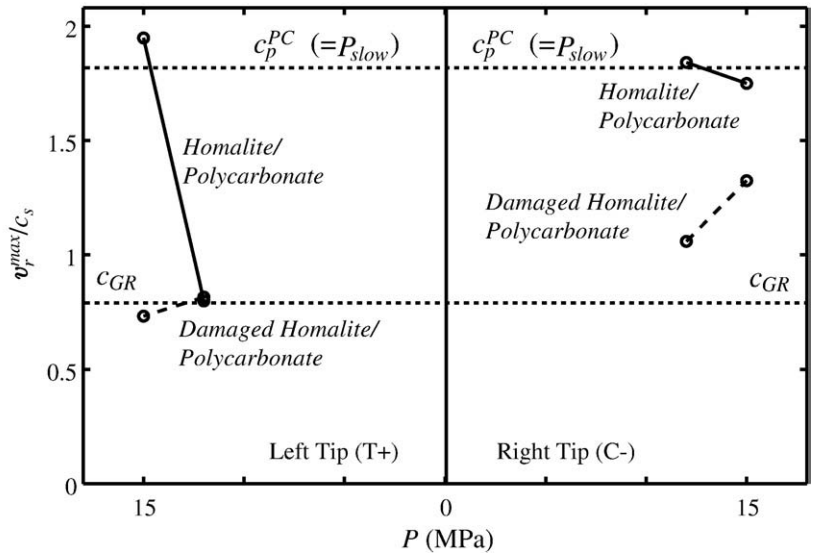

Fig. 8. The effect of load on maximum rupture velocity of a dynamic shear rupture on the interface between damaged Homalite and polycarbonate compared to velocities on the interface between undamaged Homalite and polycarbonate at the same loads. Note that damage prevents a supershear transition in the 'T+' direction but appears to only delay the acceleration toward P_{slow} in the 'C−' direction.

15 MPa (Fig. 7) the rupture in the 'T+' direction once again propagated at an average speed just below c_{GR}. However, in the 'C−' direction the rupture propagated at supershear speeds that seems to accelerate towards P_{slow}. Comparing these results with those for the undamaged bimaterial system presented earlier we see that damage has only a small affect on propagation in the C− direction but a large effect in the T+ direction. In the C− direction the rupture behaves as it did in the '−' direction in the undamaged bimaterial system where it propagated at P_{slow}. The damage had some effect in that rupture in the C− direction approaches but never quite reaches P_{slow} within our window of observation. The effect of damage is much more evident in the T+ direction where the rupture always (always close to c_{GR}) remained sub-shear while in undamaged bimaterial under the same loading conditions, propagation in the '+' direction eventually transitioned to supershear speeds that approached P_{fast}.

7. Discussion

The effects of damage on the Homalite/polycarbonate bimaterial system are summarized in Fig. 8 where the velocities for ruptures on the interface between undamaged Homalite and polycarbonate are compared with the results for damaged Homalite in contact with polycarbonate. Based on our experimental results and those in Biegel et al. (2010-this issue), we hypothesize that compression at the crack tip immobilizes the flaws comprising the damage and they do not play a significant role in dynamic propagation. This hypothesis is supported by the observation that increasing the applied load, P, does indeed lead to rupture velocities in the 'C−' direction that are similar to those in the '−' direction in the undamaged Homalite–polycarbonate system. Increasing the load increases the magnitude of off-fault compression at the crack tip leading to lesser damage activation.

The reduction in propagation velocity in the 'T+' direction is caused by a significant lowering of the dynamic elastic modulus on the damaged side of the interface due to activation of the damage by the tension, and by friction loss during sliding on the fractures that comprise the damage. When the applied load is increased to 15 MPa at the same fault angle $\alpha = 25°$, the rupture on the 'T+' side still propagates with a velocity well below the generalized Rayleigh wave speed. This significant reduction in rupture velocity, compared to the undamaged case where the velocity is approaching P_{fast}, may be due to increased damage activation at the higher applied load.

While these are still early results they nevertheless, along with Biegel et al. (2010-this issue), introduce an additional source of rupture asymmetry (or in the extreme case a favored rupture direction). For example the reason why the 2004 Parkfield earthquake ruptured in the '−' direction could be explained by our results. This of course requires the tensile side of damage, 'T', aligning with the '−' direction dictated by elastic mismatch. The 1934 and 1966 Parkfield events however propagated in the '+' direction. One possibility, and a likely one based on recent SAFOD observations, is that there are two principal slipping surfaces bounding a damaged core which in itself is bounded by a less stiffer material on one side and more stiff material on the other side as shown in Fig. 9. This is in agreement with the studies done by Thurber et al. (2003) who do indeed report a broad structure like we hypothesize, in which the two strands are separated by a distance of the order of 200m which is about 2–3R_0, the process zone length that controls the spatial extent of off-fault damage. In this case depending on where the rupture nucleates it would propagate in either direction and still remain almost unilateral.

In summary, a rupture propagating along the interface between damaged and undamaged material cannot be understood by simply accounting for the reduction in elastic stiffness caused by the damage. The interaction between stress concentration at the rupture front and

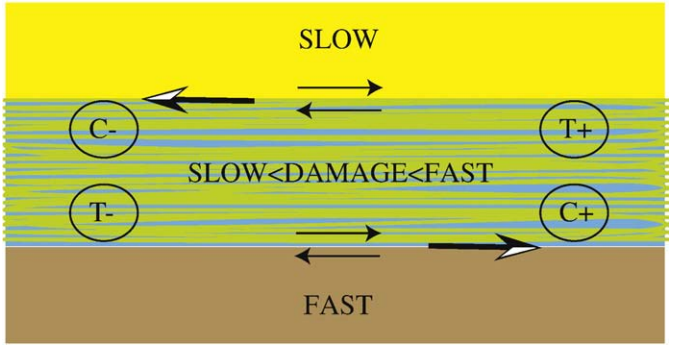

Fig. 9. One possible scenario to explain preferred rupture direction. The damaged core in the center is abutted on top by a less stiff material (labeled slow) and a more stiff material in the bottom. Large arrows indicate the direction of faster (or in some cases preferred) rupture propagation. This scenario assumes that the width of the damage zone is of the order of or larger than R_0, the size of the process zone.

Please cite this article as: Bhat, H.S., et al., The effect of asymmetric damage on dynamic shear rupture propagation II: With mismatch in bulk elasticity, Tectonophysics (2010), doi:10.1016/j.tecto.2010.03.016

the off-fault damage produces asymmetric propagation that can be opposite to that produced by velocity contrast and, in the cases studies here, with a stronger effect.

References

Adams, G.G., 1995. Self-excited oscillations of two elastic half-spaces sliding with a constant coefficient of friction. J. Appl. Mech. 62, 867–872.

Ampuero, J.P., Ben-Zion, Y., 2008. Cracks, pulses and macroscopic asymmetry of dynamic rupture on a bimaterial interface with velocity-weakening friction. Geophy. J. Int. 173. doi:10.1111/j.1365-246X.2008.03736.x.

Ben-Zion, Y., 2001. Dynamic ruptures in recent models of earthquake faults. J. Mech. Phys. Solids 49, 2209–2244.

Ben-Zion, Y., Huang, Y., 2002. Dynamic rupture on an interface between a compliant fault zone layer and a stiffer surrounding solid. J. Geophy. Res. 107 (B2).

Biegel, R.L., Sammis, C.G., Rosakis, A.J., 2008. An experimental study of the effect of off-fault damage on the velocity of a slip pulse. J. Geophys. Res. 113 (B4).

Biegel, R.L., Bhat, H.S., Sammis, C.G., and Rosakis, A.J., 2010-this issue. The Effect of Asymmetric Damage on Dynamic Shear Rupture Propagation I: No Mismatch in Bulk Elasticity, Tectonophysics: Special Volume on Supershear Ruptures.

Bouchon, M., Bouin, M.P., Karabulut, H., Toksoz, M.N., Dietrich, M., Rosakis, A.J., 2001. How fast is rupture during an earthquake? New insights from the 1999 Turkey earthquakes. Geophys. Res. Lett. 28, 2723–2726.

Cochard, A., Rice, J.R., 2000. Fault rupture between dissimilar materials— ill-posedness, regularization, and slip-pulse response. J. Geophy. Res. 105 (B11).

Coker, D., Lykotrafitis, G., Needleman, A., Rosakis, A.J., 2005. Frictional sliding modes along an interface between identical elastic plates subject to shear impact loading. J. Mech. Phys. Solids 53, 884–922.

Harris, R.A., Day, S.M., 1997. Effects of a low-velocity zone on a dynamic rupture. Bull. Seismol. Soc. Am. 87 (5), 1267–1280.

Harris, R.A., Day, S.M., 2005. Material contrast does not predict earthquake rupture propagation direction. Geophys. Res. Lett. 32 (23), L23301. doi:10.1029/2005GL023941.

Le Pichon, X., Chamot-Rooke, N., Rangin, C., Sengor, A.M.C., 2003. The North Anatolian Fault in the Sea of Marmara. J. Geophys. Res. 108 (B4), 2179. doi:10.1029/2002JB001862.

McGuire, J.J., Zhao, L., Jordan, T.H., 2002. Predominance of unilateral rupture for a global catalog of large earthquakes. Bull. Seismol. Soc. Am. 92 (8), 3309–3317.

O'Connell, R.J., Budiansky, B., 1974. Seismic velocities in dry and saturated cracked solids. J. Geophys. Res 79 (35), 5412–5426.

Prakash, V., Clifton, R.J., 1993. Time resolved dynamic friction measurements in pressure-shear, experimental techniques in the dynamics of deformable solids. Presented at the 1st Joint Mechanics Meeting of ASME, ASCE, SES, MEET'N'93, Charlottesville, Virginia, June 6–9.

Ranjith, K., Rice, J.R., 2001. Slip dynamics at an interface between dissimilar materials. J. Mech. Phys. Solids 49, 341–361.

Renardy, M., 1992. Ill-posedness at the boundary for elastic solids sliding under Coulomb friction. J. Elasticity 27 (3), 281–287.

Rice, J.R., 2001. New perspectives on crack and fault dynamics. In: Aref, H., Phillips, J.W. (Eds.), Mechanics for a New Millennium. Kluwer Academic Publishers, pp. 1–23.

Rice, J.R., Sammis, C.G., Parsons, R., 2005. Off-fault secondary failure induced by a dynamic slip pulse. Bull. Seismol. Soc. Amer. 95 (1), 109–134.

Rosakis, A.J., 2002. Intersonic shear cracks and fault ruptures. Adv. Phys. 51, 1189–1257.

Rosakis, A.J., Xia, K.W., Lykotrafitis, G., Kanamori, H., 2007. Dynamic shear rupture in frictional interfaces: speeds, directionality and modes: In: Kanamori, H. (Ed.), Treatise in Geophysics, vol. 4, pp. 153–192.

Rubin, A.M., Ampuero, J.P., 2007. Aftershock asymmetry on a bimaterial interface. J. Geophys. Res. 112, B05307. doi:10.1029/2006JB004337.

Shi, Z.Q., Ben-Zion, Y., 2006. Dynamic rupture on a bimaterial interface governed by slip-weakening friction. Geophys. J. Int. 165, 469–484.

Thurber, C., Roecker, S., Roberts, K., Gold, M., Powell, L., Rittger, K., 2003. Earthquake locations and three-dimensional fault zone structure along the creeping section of the San Andreas Fault near Parkfield, CA: preparing for SAFOD. Geophys. Res. Lett. 30 (3), 1112.

Weertman, J., 1980. Unstable slippage across a fault that separates elastic media of different elastic constants. J. Geophys. Res 85 (83), 1455–1461.

Xia, K.W., Rosakis, A.J., Kanamori, H., 2004. Laboratory earthquakes: the sub-Rayleigh-to-supershear rupture transition. Science 303, 1859–1861.

Xia, K.W., Rosakis, A.J., Kanamori, H., Rice, J.R., 2005. Laboratory earthquakes along inhomogeneous faults: directionality and supershear. Science 308, 681–684.

Please cite this article as: Bhat, H.S., et al., The effect of asymmetric damage on dynamic shear rupture propagation II: With mismatch in bulk elasticity, Tectonophysics (2010), doi:10.1016/j.tecto.2010.03.016